ISSN 2063-5346

STUDY OF HEAT AND MASS TRANSFER IN BOUNDARY LAYER FLOWS OVER A POROUS SHRINKING/ STRETCHING SHEET

Shamasuddin wani[1] R. k. Shrivastav[2]

Article History: Received: 10.05.2023 Revised: 29.05.2023 Accepted: 09.06.2023

Abstract

Changes in boundary layer flow due to suction and blowing of a non-Newtonian fluid as that fluid travels closer and closer to an exponentially increasing surface are the primary focus of this research. The behavior of fluids that are not of the Newtonian type may be defined with the help of the Casson model. The equation that is used to describe the temperature field has a variable that is meant to represent thermal radiation. "This study presents a comprehensive investigation of the flow behavior of Casson fluid over a porous stretching surface, considering the effects of heat transfer and thermal radiation. The Casson fluid model is employed to describe the non-Newtonian characteristics of the fluid, which is encountered in numerous industrial applications. The governing equations for the flow, heat transfer, and radiation are derived using the conservation laws of mass, momentum, and energy. The resulting system of nonlinear partial differential equations is solved numerically using an efficient computational method. The velocity, temperature, and concentration profiles are obtained for different values of the physical parameters involved in the problem. The analysis reveals that the velocity and temperature profiles are significantly influenced by the Casson fluid parameter, the radiation parameter, the Prandtl number, the Eckert number, and the permeability parameter. Moreover, it is observed that increasing the Casson fluid parameter leads to a reduction in the velocity profile, while an increase in the radiation parameter enhances the temperature distribution near the surface. the study examines the skin friction coefficient, the Nusselt number, and the Sherwood number to assess the heat and mass transfer characteristics of the system. The results show that the skin friction coefficient decreases with increasing Casson fluid parameter, while the Nusselt and Sherwood numbers increase with the radiation parameter. the present study provides valuable insights into the flow behavior of Casson fluid over a porous stretching surface with heat transfer and thermal radiation. The findings offer significant implications for optimizing various industrial processes involving non-Newtonian fluids and porous media". The outcomes of this research will contribute to the design and development of more efficient heat exchangers and fluid flow control systems in engineering applications. Researchers have discovered that a higher value for the suction parameter also results in a higher value for the skin-friction coefficient..

Keywords: non-Newtonian, Casson fluid, temperature.

[1]Research Scholar Dr Bhim Rao Ambedkar University Agra email sdinwani@gmail.com

[2]Professor at Agra college Agra U. P

DOI:10.48047/ecb/2023.12.11.01

1. INTRODUCTION:

The growing number of commercial applications for this phenomenon and the ensuing consequences on a broad variety of technological processes have aroused the attention of the scientific community in the study of laminar flow and heat transfer across a stretched sheet in a viscous fluid. This interest has been sparked by the expanding number of industrial uses for this phenomenon. The vast bulk of published work that is publicly accessible focuses on studies of boundary layer flow across stretched surfaces. It has been anticipated that the stretching surface's speed would grow as it moves further away from the origin that remains stationary.

After then, a large number of researchers began delving deeply into the investigation of the heat transfer properties of both Newtonian and non-Newtonian fluid flows. It was hypothesized that a flow of ferrimagnetic non-Newtonian fluid may be triggered by applying suction over a stretched surface. A number of the manufacturing processes include the utilization of non-Newtonian fluids. Non-Newtonian fluids include things like paints and oils as well as polymer suspensions, biological fluids, animal blood, colloidal solutions, and liquid crystals containing stiff molecules. Other examples include animal blood. The conventional Newtonian models of fluid dynamics are unable to account for the idiosyncrasies of these substances in an acceptable manner. It is feasible to locate a number of different models of fluids that are not Newtonian in publications that have been published. One such illustration is provided by the Casson fluid, which is a model that differentiates itself from others in a variety of respects. In this investigation, we looked at how the heat transmission characteristics of a dissipative convective Casson nanofluid were modified by a chemical reaction, a heat source, and the slip state of the nanofluid. In addition, the effects of changing the temperature of the wall on the mixed Casson nanofluid flow for a rotating sphere that was getting close to the stagnation point were investigated.

1.1 MAGNETOHYDRODYNAMICS

Magnetohydrodynamics, sometimes abbreviated as MHD, is the study of the dynamics that occur when magnetic fields interact with fluids that carry electricity. This subfield of contemporary building science is seeing a surge in research activity. Ionized quickening agents, the management of flow in atomic reactors, side-stream energy MHD pipe flows may be utilized in a broad number of contexts, including bubble levitation, generators, and fluid metal production forms, to name just a few of the numerous possibilities.When nonlinear radiation was applied, Kumar and his colleagues looked at numerous different magnetohydrodynamic (MHD) effects for non-Newtonian fluids such as Carreau, Williamson, and Micropolar fluids. They were able to do this by employing computational methods to study the MHD effects of a stretched surface operating in a porous environment.

Researchers have made tremendous headway in developing a solution for the many scientific and industrial applications of melting heat transfer. These applications include the production of semiconductors, the thawing of frozen ground, the solidification of molten rock flows, and a great many more. Utilizing a micropolar fluid enables the transmission of melting heat at the stagnation point across expanding and contracting surfaces. This is made feasible by the use of a micropolar fluid. Within the context of MHD nanofluid flow, transfer of melting heat that takes into account radiation and second-order slip. The impact of melting heat transfer on Jeffrey fluid flow towards the point where it stagnates. Additional research was carried out by scientists so that they might have a deeper

understanding of the ways in which environmental elements influenced the magnetic field.

The process of heat transmission, which is determined by thermal radiation, can be utilized in a variety of technical contexts. As illustrations of this, we may look at gas turbines and the mechanism that generates thrust in aircraft engines, in addition to missiles, nuclear power plants, satellites, and other space vehicles. Because its surface is porous in a vertical direction, it is open to convection and radiation from all directions. Radiation across a sheet that has been vertically extended, as well as stagnation point flow in MHD mixed convection. We investigate MHD flow across a flat plate, paying attention to slip, radiation, and its other potential impacts. The properties of heat radiation that were shown by Jeffrey fluid, The effect that magnetic nanoparticles have on the motion of MHD nanofluids, in which the MHD Carreau fluid is utilized in the melting process of different thicknesses.

Magneto hydrodynamics, sometimes abbreviated as MHD, is the field of study that investigates how highly conducting fluids react when placed in the presence of a magnetic field. It is possible for the flow of a conducting fluid through a magnetic field to affect not only the impact of the field but also the movement of the fluid itself through the field if it causes an electric current to be generated. It is absolutely necessary to get further knowledge regarding the fluid dynamics of electrically conducting magnetonanofluids. Magneto nanofluids are playing an important part in a variety of fields, including the creation of power generators, the treatment of conditions such as asthma and cancer, and targeted medication delivery. As a direct consequence of surface stretching, the plastics and metals sectors stand to gain a significant competitive advantage from flow. Blowing glass, continuous casting of metals, and textile spinning all utilise the flow principle in the form of a stretched sheet. The rate of heat transfer at the stretching sheet plays a crucial role in all of the aforementioned applications of flow via stretching sheet..

1.2 Fundamental sorts of Casson fluid

The passage discusses various aspects of Casson fluids and their potential applications in engineering and science. It highlights the distinguishing properties of Casson fluids, such as possessing the yield stress of a non-Newtonian fluid. One specific example mentioned is human blood, which is theorized to exhibit Casson fluid characteristics due to its chainlike structure and the presence of components like proteins, fibrinogen, and rouleaux. The passage also mentions the development of different models to study the dynamics of fluids that do not follow Newtonian equations. Two specific cases are mentioned where exact solutions have been found for the motion of Casson fluids. The first case involves peristaltic motion in an asymmetric channel containing crude oil, which is relevant to the transmission of heat and mass. The second case deals with the motion of a Casson fluid across an exponentially permeable stretched surface. Both scenarios take into account the impacts of Dufour and Soret effects, which relate to the transport of heat and mass. the passage briefly discusses the impact of size reduction on concentration and velocity boundary layers. It suggests that as the size of the case is reduced, the concentration boundary layer becomes more dense while the velocity boundary layer becomes less dense. This observation implies that size plays a significant role in the behavior of Casson fluids, and understanding these effects is important in practical applications. the passage presents an overview of Casson fluids, their properties, and their potential applications. It also highlights specific cases where exact solutions have been derived for the motion

of Casson fluids, emphasizing the relevance of these fluids in heat and mass transfer. Finally, it touches upon the impact of size reduction on concentration and velocity boundary layers, suggesting that size-dependent effects should be considered when studying Casson fluid dynamics.

2. REVIEW LITERATURE :

Sulochana et al. (2015) are the authors of this study. To be more specific, they were thinking about the dynamics of fluids. In this study, the characteristics of the flow of a casson fluid approaching the stagnation point across a stretched surface were explored, and the presence of a viscous dissipation effect was taken into consideration. This sort of heat transmission is non-uniform, and it is caused by a combination of factors, including thermal radiation, a heat source or sink that is not uniform, and fluid movement through a porous and stretched surface. This pattern has the potential to occur in the event that fluid is moving through a stretched porous surface at the same time as heat is being radiated from the surface. When the MHD flow comes to a complete standstill, the state is as follows: The behavior of nanofluids in an induced magnetic field as they travel through an area that has a stretching surface that is not isothermal.

S. Shaw, G. Mahanta(2015)In this article, we investigate this phenomena by concentrating on the motion of a magnetohydrodynamic (MHD) three-dimensional Casson fluid as it passes through a porous sheet that has been linearly stretched. A convective boundary condition is enforced at the surface of the fluid, and the thermal conductivity of the fluid varies in a linear fashion in response to temperature variations. The temperature fields and the velocity fields are both subjected to a computer analysis, during which numerous elements of each field are taken into consideration. The Spectral Relaxation Method, often known as SRM, is utilized so that answers to the pertinent governing equations may be located. It is obvious that these solutions are in good concord with both one another and the various criteria when the few possibilities that are now available are contrasted with them. We have included graphs of the velocity and temperature so that you may more readily observe the behaviors associated with the various factors. Following this point in the conversation, a chart describing the impacts of skin friction and the local Nusselt number on the various parameters is provided. The table includes detailed information.

S. Sreenadh. (2017), The influence of heat radiation on fluid motion will be extensively investigated to acquire deeper insights into the flow behavior. In this study, various parameters related to the flow, such as the concentration and temperature of the walls, as well as the stretching velocity, are expected to exhibit exponential growth within the prescribed scenario. This growth pattern arises due to the interplay between the concentration of the walls and the temperature of the walls. The application of similarity transformations simplifies the problem, enabling the identification of a solution strategy. The subsequent step involves seeking a numerical solution to the formulated problems using the bvp4c package, a commonly used component of MATLAB. The resulting equations, which describe the profiles of velocity, temperature, and concentration, are presented in the study along with graphical representations of the variables involved. These visualizations aid in understanding the components of the equations and their interactions.

After that, the bvp4c Matlab add-on is utilized in order to solve the equations that were produced. When the results of this study are compared to those of the accessible corpus of previous research, it is discovered that there is a high degree of congruence between the two sets of

findings. Due to the existence of some extremely rare situations in which the stretching parameter is negative, dual solutions for the velocity, temperature, concentration, and skin friction equations have been developed. It is conceivable that such a circumstance may arise. These options are interchangeable and can serve in place of one another in any circumstance. It was concluded that the problem could be effectively resolved using either of these two different strategies. This article provides an in-depth analysis of the impacts that the Casson parameter has on surface mass transfer, heat transfer, and friction, as well as explains how the parameter influences these processes.

3. OBJECTIVE OF THE STUDY:

1. To conduct research on Casson fluid passing through a porous stretched surface with thermal radiation.
2. To research a non-Newtonian fluid's boundary layer flow

4. METHODOLOGY:

Setting up the correlation variables by:

$$\eta = \sqrt{\frac{U_0}{2\nu L}} e^{\frac{x}{2L}} y, \quad (3.1)$$

$$u = U_0 e^{\frac{x}{2L}} f'(\eta), \quad (3.2)$$

$$\upsilon = -\sqrt{\frac{\nu U_0}{2L}} e^{\frac{x}{2L}} \{f(\eta) + \eta f'(\eta)\}, \quad (3.3)$$

$$T = T_\infty + T_0 e^{\frac{x}{2L}} \theta(\eta) \quad (3.4)$$

the governing equations are simplified to (2) and (5) when (8) is substituted in.:

$$\left(1 + \frac{1}{\beta}\right) f''' + f f'' - 2f'^2 = 0, \quad (3.5)$$

$$\left(1 + \frac{4}{3}N\right)\theta'' + \Pr(f\theta' - f'\theta) = 0 \quad (3.6)$$

Boundary conditions are expressed as follows: at

$$\eta = 0, \quad f' = 1, \quad f = S, \quad \theta = 1, \quad (3.7)$$

$$\eta \to \infty, \quad f' \to 0, \quad \theta \to 0 \quad (3.8)$$

where the prime indicates a degree of difference with regard to η, $S = \frac{V_0}{\sqrt{\frac{\nu_0}{2L}}} > 0$ (or < 0) is the parameter that measures suction (or blowing), $N = \frac{4\sigma T_\infty^3}{\kappa k^*}$ i is the radiation parameter, $\Pr = \frac{\mu c_p}{\kappa}$ is the Prandtl number.

5. NUMERICAL METHOD

It is feasible to find a solution for each of the equations if one first converts the equations that came before it (9) and (10) into an initial value problem and then adds the boundary conditions (11), (12). In this manner, it is possible to find a solution for each of the equations. We set:

$$f' = z, z' = p, \theta' = q, \quad \textbf{(3.9)}$$

$$p' = (2z^2 - fp)/\left(1 + \frac{1}{\beta}\right), \quad \textbf{(3.10)}$$

$$\theta' = q, q' = -\left(\frac{3\Pr}{4N + 3}\right)(fq - z\theta) \quad \textbf{(3.10)}$$

We need a value for the parameter p(0) so that we may integrate equations (13) and (14), which both have an initial value issue. This might also be stated as: f'' (0) and $\theta'(0)$. The border, on the other hand, does not supply any values of this nature. The selection of appropriate finite values for the firing technique is the single most important but also one of the most difficult components. η_∞. In order to determine η_∞ In order to find a solution to the problem of finding boundary values that is presented by equations (13)–(15), we must first select an initial estimate value for a particular set of physical parameters. Because of this, we are able to deduce. f''0) and h/ (0). The method for resolving the issue is carried out once more, this time with an additional substantial value of

η_∞ until two consecutive values of were reached. f'' (0) and $\theta'(0)$ only differ by the significant digit that has been supplied. The most recent value for η_∞ is finally chosen to serve as the limit value g1 because it offers the optimal level of compatibility with the specific set of criteria that is under consideration. The relevance of the fact that η_∞ may be vary depending on the particular set of physical elements being considered. Taking into account the infinitesimal value of η_∞ When a conclusion has been reached regarding this matter, the integration will proceed. We investigate the discrepancies that exist between the calculated values for f'' and θ at $\eta = 10$ taking into account the existing boundary conditions f'' $\theta(10) = 0$ and $\theta'(0)$ and make any adjustments to the predicted values, $f''0)$ and $\theta'(0)$ with the purpose of providing an estimate that is more precise for the solution. The progression of the values is what we assume as given. f'' (0) and $\theta'(0)$ In addition to that, you need to make use of the Runge–Kutta algorithm of the fourth order with a step size of 0.01. The procedures described above are repeated multiple times until we reach a level of precision that we deem to be adequate. 10^{-5}.

6. RESULTS AND DISCUSSIONS

The verification of the results

The importance of the absent beginning condition will be investigated as part of the process of determining how well the program was put to use.. $f''(0)$ while using a Newtonian fluid as an example $(\beta = 0)$ is contrasted with the ideals that were documented in the pioneering work that they carried out, as well as the discoveries that were made as a result of their endeavors.. $f''(0)$ = 1.281812to within six digits of decimal accuracy, which is in reasonable accord with the $f''(0)$ = 1.28180, $f''(0)$ = 1.28181, and $f''(0)$ = 1.281811, assuming that we can trust even just one of those sources. To evaluate the accuracy of the numerical scheme employed in the study, a comparison is made between the obtained results and the corresponding values of the heat transfer coefficient. This comparison serves as a crucial step in assessing the reliability of the numerical model. By comparing the calculated heat transfer coefficient with known values or experimental data, the researchers can gauge the accuracy and validity of their numerical approach.

The primary objective of this comparison is to verify whether the numerical model yields accurate results in predicting the heat transfer coefficient. If the numerical scheme produces results that closely align with the expected values, it provides confidence in the reliability and accuracy of the computational methodology employed. On the other hand, significant deviations between the calculated and expected heat transfer coefficients may indicate the presence of errors or limitations in the numerical model, prompting further investigation and potential refinements.

By carrying out this comparison, researchers can ascertain the correctness and fidelity of the numerical scheme utilized in predicting the heat transfer coefficient. The accuracy assessment provides valuable insights into the reliability of the numerical model, enabling researchers to make informed conclusions about the validity of their findings and the overall accuracy of the computational approach employed in the study. $[-\theta'(0)]$

A comprehensive analysis is conducted for the scenarios involving a Newtonian fluid with no suction or blowing at the boundary (S = 0) and for cases with N = 0 (representing absence of chemical reaction) using the available published data. The results of this analysis are presented in Table 1, which can be found

further down on the page.Table 1 encompasses various specific scenarios and includes other notable examples for comparison. The outcomes indicate a significant level of agreement between the two groups of results, suggesting consistency and coherence.Furthermore, a thorough comparison is performed between the findings obtained in this study and those corresponding to the values of the heat transfer coefficient. This comparison serves as a means to assess the accuracy and reliability of the obtained results. By scrutinizing the agreement between the present results and the established values, researchers can determine the validity and correctness of the heat transfer predictions.Through this comparative analysis and evaluation of the heat transfer coefficient, researchers gain valuable insights into the accuracy and reliability of their findings. This process reinforces the confidence in the obtained results and allows for informed conclusions regarding the effectiveness of the computational methodology employed in predicting heat transfer behavior... $[-\theta'(0)]$ the Eckert number (E), a computation was performed utilizing the available numerical results provided by Bidin and Nazar [10], as well as the analytical findings published by Nadeem et al. [14]. Both sets of results were incorporated into the calculation process. This step was essential to determine the Eckert number accurately. The outcomes of this computation, performed with S (suction or blowing) set to 0, covering a range of different values of the thermal radiation parameter (N), are summarized in Table 2, located further down on the page. The results presented in Table 2 demonstrate that there is a significant level of agreement and common ground between the two groups of findings. This convergence between the numerical and analytical approaches reinforces the validity and reliability of the conclusions drawn from the study. It further strengthens the credibility of the obtained results and lends support to the overall findings of the research.

.

Table 1 Values of $[-\theta'(0)]$ when applied to a Newtonian fluid where the Prandtl number can take on a wide variety of values.

Pr	Elbashbeshy EMA [2]	Aksoy Y [10]	Fung YC [12]	Mukhopadhyay S [15]	$S = 0, N = 0$
1	.8548	.8547	.8548	.8548	.8547
2		1.714		1.3715	1.3714
3	1.7691	1.7691	1.7691	1.691	1.7691
4	1.4001		2.4001	2.4001	2.4001
5	2.5604		3.5604	3.5604	3.5603

Table 2 Values of $[-\theta'(0)]$ For Newtonian fluids, considering different Prandtl number values, and in the presence of heat radiation.

Pr	Pakdemirli M [10] conducted their experiment with E equal to 0 (for two different values of the radiation parameter K).			For the PEST scenario described in Nadeem et al. [14], in which E = 0, k1 = 0, B = 0, and w = 0 (for			This research will be presented with S equal to 0 (for two different values of the radiation parameter N).		
	.5	1.0		.5	1.0		.5	1.0	
1	0.6765	0.5715		0.690	0.544		0.6765	0.5116	
2	1.0735	0.8627		1.073	0.863		1.0734	0.8626	
3	1.3807	1.1214		1.381	1.121		1.3807	1.1213	

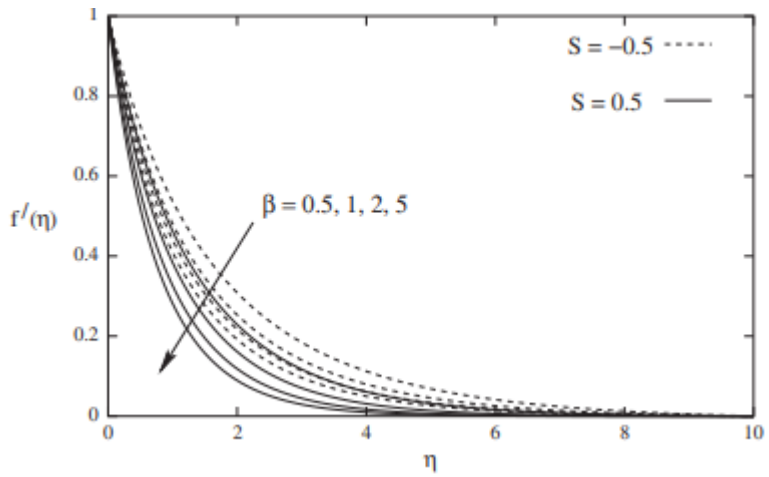

Fig 1 profiles of velocities for a variety of various setting combinations of the Casson parameter β in the presence of blowing and suction.

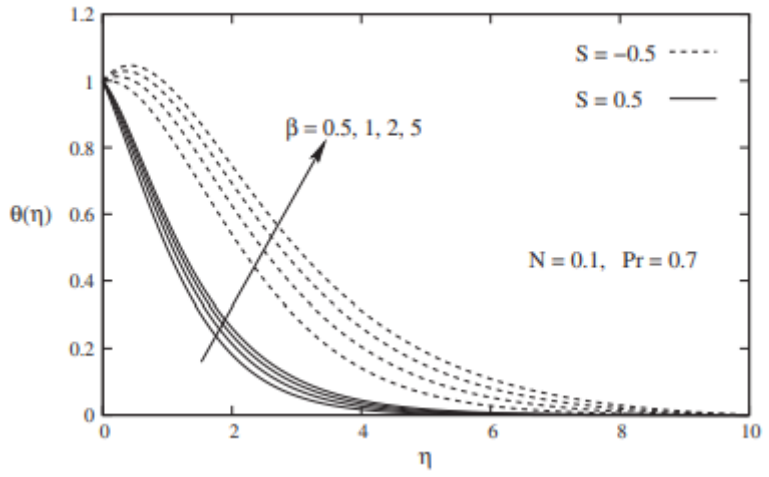

Fig 2b Casson parameter profiles of temperatures for an object variety of different values β within the context of air movement and vacuuming.

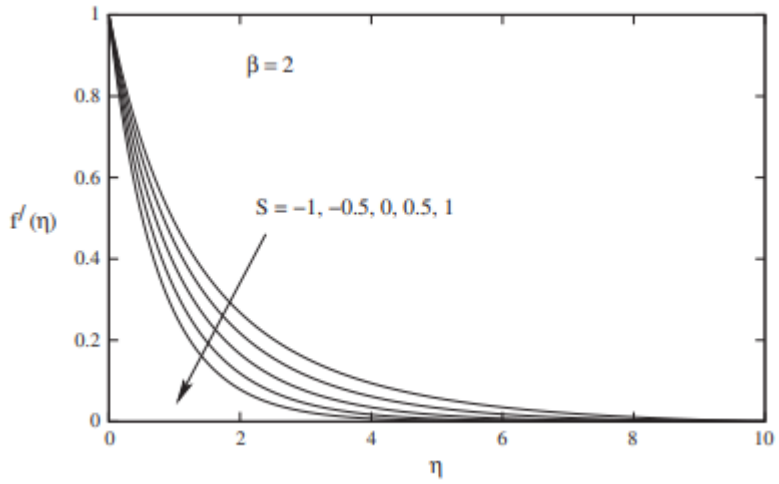

Fig 3a different suction and blowing parameter S values, together with their corresponding velocity profiles.

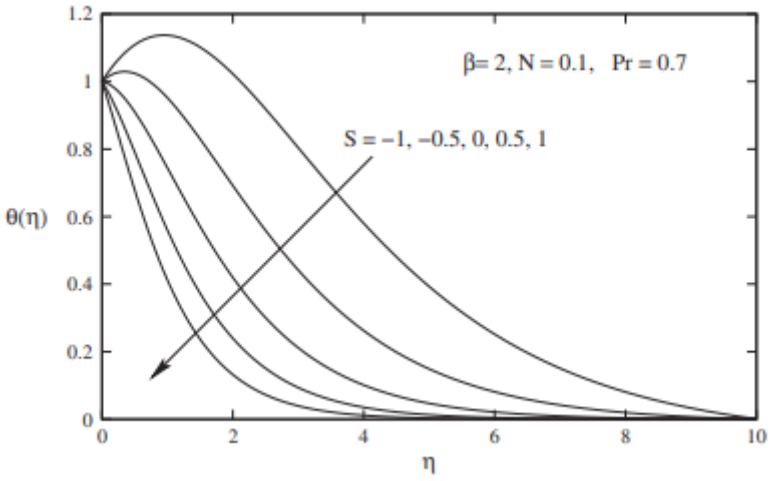

Fig 3b There are several temperature profiles for a single value of the suction/blowing parameter S.

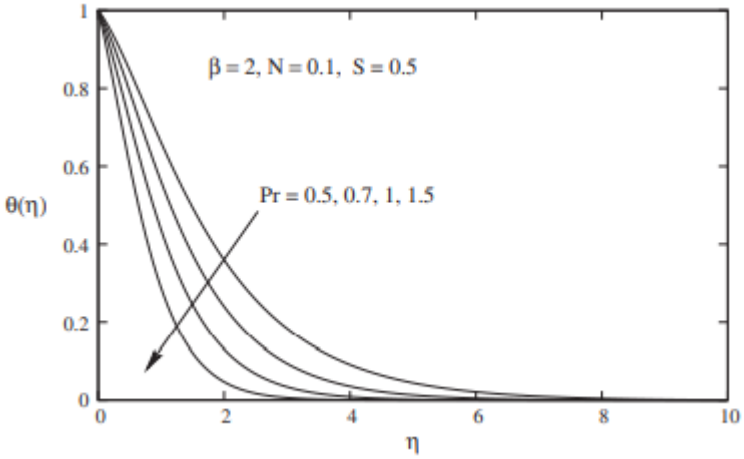

Fig 4a: Temperature distributions throughout the presence of suction over a wide range of various Prandtl values

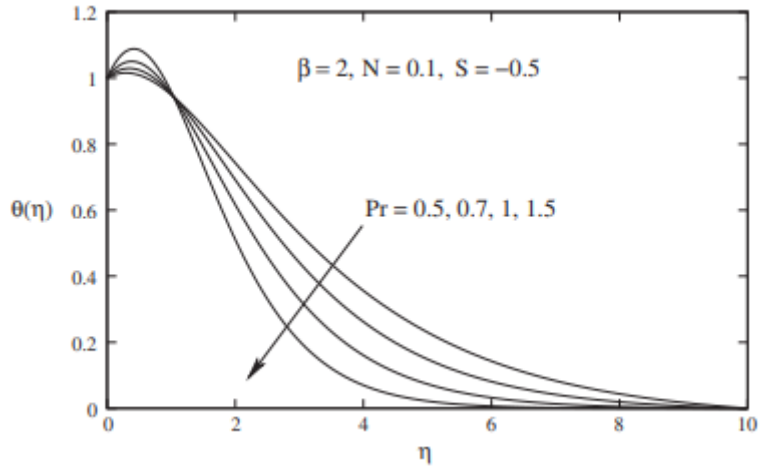

Fig 4b Temperature distributions for a variety of different Prandtl values while there is blowing in the environment.

7. TEMPERATURE AND FLOW RESULTS FROM DIFFERENT PHYSICAL PARAMETERS

The methodology described in the prior section has been utilized in the execution of numerical simulations, and the outcomes of these simulations have been examined. During the course of the calculations, a wide variety of Casson parameter settings were examined and evaluated.. β parameter S for suction and blowing, parameter N for radiation, and parameter Pr for the Prandtl number. In order to better illustrate the findings, numerical values have been presented in Figs respectively.

First, let's have a look at how the Casson parameter affects things. β about the temperature and the patterns of the velocity. The influence that the Casson parameter b has on the velocity profiles of permeable sheets is seen in Fig. 2a. It has been established that a decrease in velocity results from raising the value of the Casson parameter.. β. a change in the characteristics of the thickness of the momentum boundary layer in response to a rise in β a valid point that should be brought up. When the fluid velocity is slowed down as a result of suction (S = 0.5), the effect is notably more noticeable than when it is slowed down as a result of blowing (S = 0.5). (Fig. 2a)

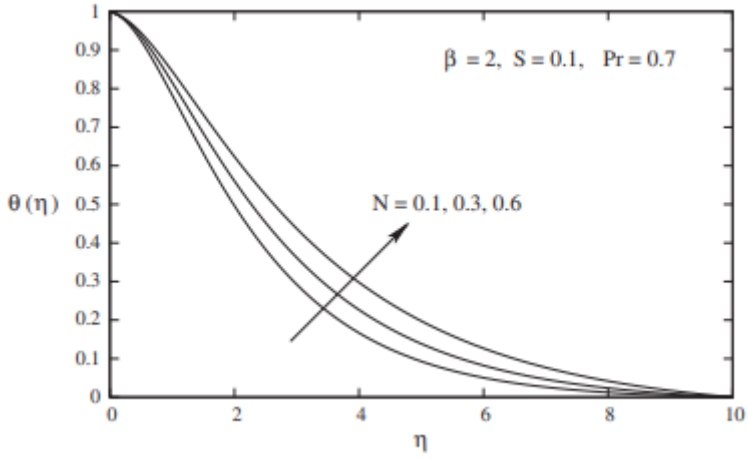

Fig 5 There are several distinct temperature profiles for each of the possible values of the radiation parameter N.

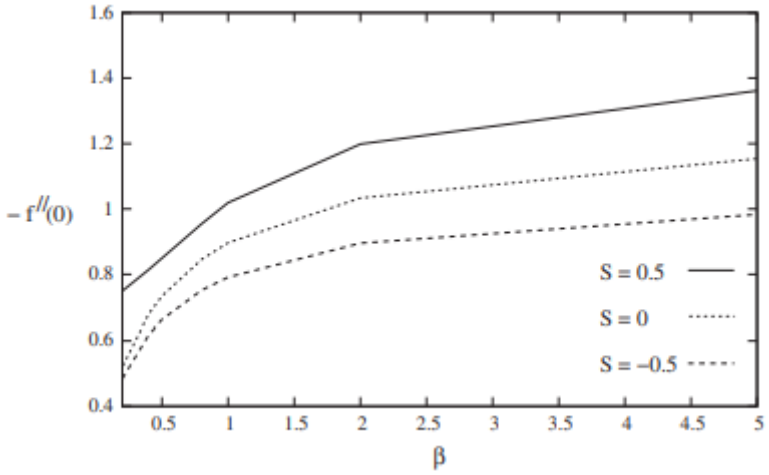

Fig 6a $f''(0)$ versus Casson parameter β when the suction/injection parameter S is set to three different values.

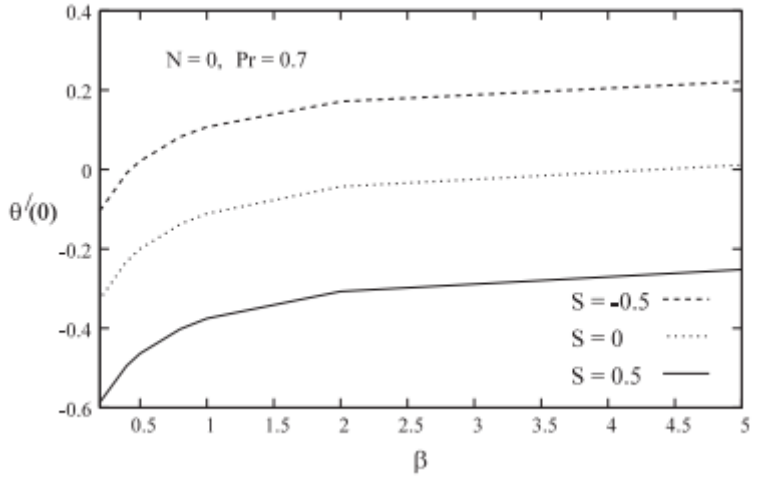

Fig 6b gradient in wall temperature $\theta'(0)$ compared to the Casson parameter β for the suction/injection parameter S's three possible values.

The temperature profile characteristics of a permeable stretched sheet are depicted in Fig 2b for a variety of settings that have been tried and tested for the Casson parameter b. "The temperature in that area has increased as a direct result of the circumstance. As a consequence of the change in b, the thickness of the thermal boundary layer increases.. In the case where there is blowing (S = 0.5), the rise in temperature over the whole field is noticeably more significant than in the case where there is suction (S = 0.5) (Fig. 2b). In the event that there is wind, the temperature will rise to an unsafe level (Fig. 2b). It has been shown that the suction and blowing parameter S has an effect on the velocity profiles of an exponentially stretched sheet (Fig. 3a), and this effect can be seen in the Fig. It has been established that there is a substantial rise in the velocity of the fluid when it is blown, but there is a large decrease in the velocity of the fluid when the suction is increased (Fig. 3a). It has been demonstrated that the thickness of the boundary layer is reduced when wall suction is taken into account (S > 0), and that this results in a slowing impact on the velocity field. This occurs as a direct consequence of the boundary layer sucking in less air as a direct result of the walls. As

a result, the boundary layer is now thinner". The value S = 0 is used to represent non-porous sheets that have been stretched, and this value indicates that the sheets are in a state of tension. On the other hand, when a person blows (S 0), they behave in the opposite manner. The stronger the blowing, the farther away from the wall the hot fluid is forced as it is pushed further away. Because viscosity has less of an effect in this area, the flow is being forced forward at a faster rate. This is where the physiological foundation for such behavior may be found. This impact has directly contributed to an increase in the highest potential speed that may be achieved within the boundary layer. When it comes to suction, the same idea applies; the only difference is that the direction is reversed. Fig 3b displays the temperature profiles that are produced while varying the value of the suction/blowing parameter S. It has been demonstrated that raising the degree of suction results in a decrease in temperature (Fig. 3b), but increasing the level of blowing results in an increase in temperature. The The existence of a breeze (Fig. 3b) should be carefully observed since it will raise the temperature. The application of suction causes a process that directly results in a significant reduction in the temperature field's amplitude. The velocity and temperature of the boundary layer are actually dispersed more evenly across the layer due to suction. This happens all along the boundary layer. It is conceivable to draw air from the surroundings of the structure to accomplish this purpose. By drawing air from the environment just around the instrument, this is accomplished. Fluid suction acting on a surface typically leads to the narrowing of both the thermal and hydrodynamic boundary layers. This phenomenon occurs due to the boundary layer's ability to regulate the response of its thickness to temperature variations. When the boundary layer is relatively shallow, the influence of viscosity becomes more prominent compared to other factors. As the temperature decreases within the boundary layer, the effects of viscosity become more pronounced, causing a reduction in fluid movement. This reduction in flow velocity is a direct consequence of the decreased temperature. The introduction of fluid suction enhances the thickness of the thermal boundary layer. Consequently, this increase in thickness slows down the rate at which heat is transferred throughout the system. The expansion of the thermal boundary layer, as observed in the study, serves as supporting evidence for this claim. Overall, the narrowing of the thermal and hydrodynamic boundary layers due to fluid suction is attributed to the interplay between temperature variations, viscosity, and the boundary layer thickness. Understanding these dynamics is essential for optimizing heat transfer processes and designing efficient systems where fluid suction plays a significant role..

The temperature profile is significantly influenced by the Prandtl number Pr when there is suction at the boundary and the suction value is 0.5, as illustrated in Fig 4a. When there is suction at the border, this is the situation. This is the condition that exists when there is suction. It has been demonstrated that higher levels of Pr are associated with lower temperatures as opposed to higher temperatures. Continuing with the analysis, it is plausible that the trend of the thermal boundary layer thinning out will persist even as the Prandtl number continues to rise. The Prandtl number, defined as the ratio of momentum diffusivity to temperature diffusivity, provides valuable insight into this relationship. Interestingly, such an outcome would be a remarkable and unexpected turn of events.

To describe this connection more precisely, a numerical value can be employed. In the context of heat transmission-related issues, the Prandtl number (Pr) serves as a crucial parameter for adjusting the thickness of both the momentum and thermal boundary

layers. When the Prandtl number is low, the thermal boundary layer for liquid metals, for instance, tends to be significantly thicker than the momentum boundary layer. This discrepancy arises due to the temperature difference existing between the thermal and momentum boundary layers.

The reason behind this distinction lies in the dissipation of heat at a rate that is considerably faster than the velocity (or momentum) in the system. This leads to the formation of a thermal boundary layer. In such scenarios, the temperature experiences more significant variations compared to the momentum, resulting in a thicker thermal boundary layer. The increasing Prandtl number indicates a rising influence of temperature diffusivity relative to momentum diffusivity. Consequently, the thermal boundary layer becomes thinner compared to the momentum boundary layer. This counterintuitive behavior challenges conventional expectations where a higher Prandtl number would typically correspond to a thicker thermal boundary layer. Understanding this intricate relationship between the Prandtl number and the thickness of boundary layers is crucial for accurately predicting and manipulating heat transfer phenomena. Further investigations and analyses are necessary to explore the underlying mechanisms and identify the specific conditions under which this phenomenon occurs. By deepening our comprehension of these dynamics, engineers and scientists can enhance their ability to optimize thermal processes and design efficient heat transfer systems.

When the Prandtl number Pr is large in relation to the fluid's velocity (momentum), heat convection moves at a pace akin to that of a snail. On the other hand, fluids with lower Prandtl values allow heat to leave the sheet more slowly than fluids with higher thermal conductivities. This is due to the greater thermal boundary layer structures that are present in fluids with higher thermal conductivities. This is because the observed phenomena results from larger thermal boundary layer structures, which are produced when thermal conductivities increase. As a result, the Prandtl number may be used as a tool to speed up the pace at which cooling happens in conducting flows. Fig 5b's temperature profiles show fascinating patterns over a wide range of Prandtl values when blowing is present (S = 0.5). The temperature profiles may have these properties. These patterns may be observed in a wide variety of different ranges. These temperature profiles are presented in a number of value intervals for your viewing pleasure. This astonishing finding was uncovered after an unusual characteristic in the temperature field was spotted and analyzed. There may be a discernible dip in temperature that occurs throughout the process of moving from one temperature profile to the next. It has been demonstrated that the temperature rises rapidly close to the wall (just before the point where it crosses over), but it falls with increasing distance from the wall (after the point where it crosses over) (Fig. 4b). This is due to the fact that the wall loses its insulating characteristics as you cross the threshold. If there is an abnormally rapid increase in temperature, this indicates that the maximum temperature of the fluid has been attained in a region other than merely on its surface. This is because the overshoot takes place at the layer that is the most directly exposed to the environment. The larger temperature gap between the wall and the fluid that surrounds it increases as the wall is stretched, as seen by the greater peak temperature. This is an important consideration that must be given. The acceleration of the process of heat transfer from the surface to the fluid is caused by a rise in the temperature gap that exists between the surface and the fluid in the environment that surrounds it. This

temperature gap is the driving force behind the process. Upon further investigation, it is possible to uncover a contrasting pattern that runs in the opposite direction. This can be observed by analyzing Figure 4b, where an increase in the Prandtl number leads to a thinning of the thermal boundary layer, consequently causing a decrease in its thickness. It is noteworthy that this phenomenon occurs regardless of the temperature present within the wall. Regardless of the specific temperature values, there is always a positive temperature gradient between the wall and the interior region. This counterintuitive behavior challenges conventional assumptions and highlights the complex nature of heat transfer dynamics, necessitating further exploration and analysis.

Table 3 Values of η_δ and $\eta_{\delta h}$ has a suction/blowing parameter S that may be adjusted and a variety of Casson parameters to choose from

$N = 0$, $\Pr = 0.7$.

β	η_δ				$\eta_{\delta h}$		
	$S = -0.5$	$S = 0$	$S = 1.5$		$S = -0.5$	$S = 0$	$S = 0.5$
1.2	7.08	7.69	7.34		6.63	5.51	5.68
1.5	7.24	6.38	7.44		6.03	6.37	5.24
1.7	6.49	5.60	6.63		6.71	6.96	5.55
1.5	6.25	5.27	65.27		6.99	7.19	5.79
3.0	5.65	6.50	5.35		98.62	7.80	6.17
5.5	5.19	5.94	5.79		9.05	9.30	6.50

Prandtl digit A strictly physical interpretation of the phenomena says that heat is continually moving from the fluid around the surface to the surface itself. The walltemperature gradient, shown by the notation h/(0), increases when the Pr is increased. Fig 5 illustrates how thermal radiation affects temperature profiles. It has been demonstrated that a rise in the radiation parameter N causes a rise in temperature, as seen in Fig 5. This connection is obvious. This result agrees with the observation that raising N causes the thermal boundary layer's thickness to grow, according to Abdallah [35]. The element of the effect that radiation has on the thermal boundary layer that is represented by equation number 5 is an increase in the thermal diffusivity. $\Pr/(1+\frac{4}{3}N)$ in Equation (10) has the potential to be regarded as an effective Prandtl number, and it demonstrates a diminishing trend with increasing values of N. This is because it has a negative slope. Fig. 6a illustrates some of the properties that can be found in.. $f''(0)$ related with the coefficient of skin friction and the Casson parameter b for three distinct values of the suction/blowing parameter S. the Casson parameter b is associated with the value of the suction/blowing parameter S. This is the location of it. that $[-f''(0)]$ grows as a result of β In addition to the fact that it is better for sucking than it is for blowing, it also

has the property of being able to expand. Simply taking a glance at this image should make it abundantly clear that the shear stress at the wall is really negative at this particular position. An indicator that is symptomatically not favorable for, $f''(0)$ whereas a positive sign implies that the fluid is pushing on the surface rather than the surface pulling on the fluid, shows that the surface is pulling on the fluid. “Fig 6b illustrates the features of the heat transfer coefficient.. $[\theta'(0)]$ pertaining to the framework of the Casson parameter β. The Casson parameter, denoted as b, plays a crucial role in determining the heat transfer coefficient in various flow scenarios. An increase in the value of b corresponds to an increase in the heat transfer coefficient. This parameter is indicative of both the momentum and thickness of the thermal boundary layer. When blowing occurs, the wall-temperature gradient increases, implying a higher rate of heat transfer due to enhanced momentum and reduced thermal boundary layer thickness. Conversely, when sucking is present, the wall-temperature gradient decreases significantly, indicating a reduced heat transfer rate due to diminished momentum and an increased thickness of the thermal boundary layer. The Casson parameter, therefore, offers insights into the combined effects of momentum and thermal boundary layer characteristics on heat transfer. .. δ and δ_h, respectively, and are defined similarly as the values of the dimensionless distance g from the surface at which the dimensionless velocity and dimensionless temperature h fell to 0.001 when compared with the starting values of those quantities.. The heights of the border layers in millimeters δ and δ_h are defined as $\delta = \eta_\delta \sqrt{\frac{\nu}{U_0}}$ and $\delta_h = \eta_{\delta_h} \sqrt{\frac{\nu}{U_0}}$. The dimensionless thicknesses η_δ and $\eta_{\delta h}$ Table 3 provides data on the heat transfer coefficient for different values of the suction/blowing parameter S, specifically in scenarios where thermal radiation is absent. Upon analyzing the table, it becomes evident that an increase in the Casson parameter corresponds to a decrease in the thickness of the momentum boundary layer. In other words, as the Casson parameter rises, the momentum boundary layer becomes thinner. This relationship implies that a higher Casson parameter enhances the flow's ability to transfer momentum close to the solid surface, resulting in a reduction of the boundary layer thickness. This phenomenon highlights the influence of the Casson parameter on the momentum boundary layer and its significance in understanding the fluid dynamics and heat transfer characteristics of the system. β in addition to this, when the values of the suction/blowing parameter S are increased. On On the other hand, the thickness of the thermal barrier is an important consideration. β layer thickens with an increase in the Casson parameter, but it thins down when the values of the suction/blowing parameter S are increased”.

8. CONCLUSION

The continuous flow of a Casson fluid and the transfer of heat through an increasingly porous and stretched surface are the primary foci of the investigation into this subject that is carried out using numerical methods. The presence of heat enables us to carry out this experiment successfully. The investigation at hand focuses on studying the continuous flow behavior of a Casson fluid and analyzing the heat transfer process across a surface that becomes progressively more porous and stretched. To accomplish this, numerical methods are employed to simulate the phenomena. The presence of heat is a crucial factor for the successful execution of this experiment. Presented below is an expanded summary of the significant findings derived from this study: One of

the key observations resulting from the modification of the system is that an increase in the Casson parameter enhances the robustness of the thermal boundary layer. Simultaneously, the modification adversely affects the robustness of the momentum boundary layer. This can be attributed to the fact that an elevated Casson parameter leads to the development of a thicker thermal boundary layer, which subsequently influences the dynamics of the system. Furthermore, when the suction parameter is decreased, it causes a reduction in the velocity field within a viscous incompressible fluid. As a consequence, the skin-friction coefficient increases. This effect creates a positive feedback loop, leading to further escalation in the skin-friction coefficient. Notably, when comparing the scenarios of blowing and sucking on the same surface, the skin-friction coefficient is significantly higher during suction. The presence or absence of such suction or blowing scenarios creates a stark contrast in the outcomes. Examining the behavior of the Casson parameter, it is observed that an increase in its value correlates with a corresponding rise in the shear stress at the surface. This relationship suggests the possibility of similar phenomena occurring in other scenarios as well. In addition, as the Prandtl number progressively increases, both the temperature and the thickness of the thermal boundary layer decrease. This decreasing trend continues until the Prandtl number reaches its maximum value. It is worth noting that the variation of a specific variable affects the Prandtl number, causing it to rise in tandem with the increase in the variable's value. Regarding the radiation parameter, elevating its value to higher levels results in an increase in temperature and the total amount of radiation emitted. Consequently, the intensity of the radiation also rises. The primary driving factor behind this phenomenon is believed to be the augmented effective thermal diffusivity. By expanding upon these findings, a comprehensive understanding of the intricate dynamics involved in the continuous flow of Casson fluids and heat transfer processes across porous and stretched surfaces is achieved. These insights pave the way for further advancements in related research areas and applications in various engineering and scientific fields.

9. REFERENCES

1. Magyari E, Keller B. Heat and mass transfer in the boundary layers on an exponentially stretching continuous surface. J Phys D: Appl Phys 1999;32:577–85.
2. Elbashbeshy EMA. Heat transfer over an exponentially stretching continuous surface with suction. Arch Mech 2001;53:643–51.
3. Bidin B, Nazar R. Numerical solution of the boundary layer flow over an exponentially stretching sheet with thermal radiation. Eur J Sci Resc 2009;33(4):710–7.
4. Bararnia H, Gorji M, Domairry G, Ghotbi AR. An analytical study of boundary layer flows on a continuous stretching surface. Acta Appl Math 2009;106:125–33. http://dx.doi.org/10.1007/ s10440-008-9286-3.
5. El-Aziz MA. Viscous dissipation effect on mixed convection flow of a micropolar fluid over an exponentially stretching sheet. Can J Phys 2009;87:359–68.
6. Pal D. Mixed convection heat transfer in the boundary layers on an exponentially stretching surface with magnetic field. Appl Math Comput 2010;217:2356–69.
7. Nadeem S, Zaheer S, Fang T. Effects of thermal radiation on the boundary layer flow of a Jeffrey fluid over an exponentially stretching surface. Num Algor 2011. http://dx.doi.org/10.1007/

s11075-010-9423-8.

8. Ishak A. MHD boundary layer flow due to an exponentially stretching sheet with radiation effect. Sains Malaysiana 2011;40:391–5.
9. Sahoo B, Poncet S. Flow and heat transfer of a third grade fluid past an exponentially stretching sheet with partial slip boundary condition. Int J Heat Mass Transfer 2011;54:5010–9
10. Aksoy Y, Pakdemirli M, Khalique CM. Boundary layer equations and stretching sheet solutions for the modified second grade fluid. Int J Eng Sci 2007;45:829–41.
11. Hayat T, Awais M, Sajid M. Mass transfer effects on the unsteady flow of UCM fluid over a stretching sheet. Int J Mod Phys B 2011;25:2863–78.
12. Fung YC. Biodynamics circulation. New York Inc.: SpringerVerlag; 1984.
13. Dash RK, Mehta KN, Jayaraman G. Casson fluid flow in a pipe filled with a homogeneous porous medium. Int J Eng Sci 1996;34(10):1145–56.
14. Mukhopadhyay S. Unsteady boundary layer flow and heat transfer past a porous stretching sheet in presence of variable viscosity and thermal diffusivity. Int J Heat Mass Transfer 2009;52:5213–7.
15. Mukhopadhyay S. Effects of slip on unsteady mixed convective flow and heat transfer past a porous stretching surface. Nucl Eng Des 2011;241:2660–5.
16. Mukhopadhyay S, Vajravelu K. Effects of transpiration and internal heat generation/absorption on the unsteady flow of a Maxwell fluid at a stretching surface. ASME J Appl Mech 2012;79(July):044508.
17. Mukhopadhyay S, Bhattacharyya K, Layek GC. Steady boundary layer flow and heat transfer over a porous moving plate in presence of thermal radiation. Int J Heat Mass Transfer 2011;54:2751–7.
18. Mustafa M, Hayat T, Pop I, Aziz A. Unsteady boundary layer flow of a Casson fluid due to an impulsively started moving flat plate. Heat Transfer-Asian Resc 2011;40(6):563–76.
19. Brewster MQ. Thermal radiative transfer properties. John Wiley and Sons; 1972.
20. Bhattacharyya K. Boundary layer flow and heat transfer over an exponentially shrinking sheet. Chin Phys Lett 2011;28(7):074701.
21. Abdallah IA. Analytic solution of heat and mass transfer over a permeable stretching plate affected by chemical reaction, internal heating, Dufour–Soret effect and hall effect. Therm Sci 2009;13(2):183–97.
22.] Andersson HI, Dandapat BS. Flow of a power law fluid over a stretching sheet. Appl Anal Continuous Media 1992;1:339–47.
23. Hassanien IA. Flow and heat transfer on a continuous flat surface moving in a parallel free stream of power-law fluid. Appl Model 1996;20:779–84.
24. Sadeghy K, Sharifi M. Local similarity solution for the flow of a ‘second-grade’ viscoelastic fluid above a moving plate. Int J Nonlinear Mech 2004;39:1265–73.
25. Serdar B, Salih Dokuz M. Three-dimensional stagnation point flow of a second grade fluid towards a moving plate. Int J Eng Sci 2006;44:49–58.
26. Sajid M, Hayat T, Asgharm S. Non-similar analytic solution for MHD flow and heat transfer in a third-order fluid over a stretching sheet. Int J Heat Mass Transfer 2007;50:1723–36.
27. Sajid M, Ahmad I, Hayat T, Ayub M. Unsteady flow and heat transfer of a second grade fluid over a stretching

sheet. Commun Nonlinear Sci Num Simul 2009;14:96–108.

28. Ali F. M., R. Nazar, N. M. Arfin, I. Pop (2011). MHD stagnation-point flow and heat transfer towards stretching sheet with induced magnetic field, Appl. Math. Mech. – Engl. Ed., 32(4), 409-418.
29. Chiu-On Ng (2013). Combined pressure-driven and electrosmotic flow of casson fluid through a slit microchannel, J. Non-Newtonian Fluid Mech. 198, 1-9.
30. Cortell R., (2014). Fluid flow and radiative nonlinear heat transfer over a stretching sheet, Journal of King Saud University-Science 26, 161-167.
31. Hayat T., T. Muhammad, A. Alsaedi and M. S. Alhuthali, (2015). Magnetohydrodynamic three-dimensional flow of viscoelastic nanofluid in the presence of nonlinear thermal radiation, Journal of Magnetism and Magnetic Materials 385, 222-229
32. Hayat T., Z. Nisar, B. Ahmad and H. Yasmin, (2015a). Simultaneous effects of slip and wall properties on MHD peristaltic motion of nanofluid with Joule heating, Journal of Magnetism and Magnetic Materials 395, 48-58.
33. Jayachandra Babu, M., Radha Gupta, N.Sandeep. (2015). Effect of radiation and viscous dissipation on stagnation-point flow of a micropolar fluid over a nonlinearly stretching surface with suction/injection. Journal of Basic and Applied Research International 7(2), 73-82.
34. Mustafa M, Tasawar Hayat, Ioan Pop, Awatif Hendi, (2012). Stagnation-point flow and heat transfer of a casson fluid towards a stretching sheet, Z. Naturforsch. 67, 70-76.
35. Mustafa M., A. Mushtaq, T. Hayat and B. Ahmad, (2014). Nonlinear radiation heat transfer effects in the natural convective boundary layer flow of nanofluid past a vertical plate: A numerical study, PLoS One doi:10.1371/journal.pone.e0103946
36. Mohan Krishna P, Sugunamma V and Sandeep N (2013). Magnetic field and chemical reaction effects on convective flow of a dusty viscous fluid, Communications in Applied Sciences. 1, 161-187.
37. Mohan Krishna P, Sugunamma V, Sandeep N (2014). Radiation and magneticfield effects on unsteady natural convection flow of a nanofluid past an infinite vertical plate with heat source, Chemical and Process Engineering Research, Vol 25, pp39-52.
38. Mohan Krishna P., N.Sandeep, V.Sugunamma. (2015) Effects of radiation and chemical reaction on MHD convective flow over a permeable stretching surface with suction and heat generation. Walaliak Journal of Science and Technology, 12(9), 831-847.
39. Pal D. (2011). Combined effects of non-uniform heat source/sink and thermal radiation on heat transfer over an unsteady stretching permeable surface, I. J. Communications in Nonlinear Science and Numeric. Simula. 16(4), 1890-1904.
40. Pal, D., and Mandal, G. (2015). MHD convective stagnation-point flow of nanofluids over a non- isothermal stretching sheet with induced magnetic field, Meccanica. 1-13.